

Retrofit of a 500 kA cell design into a 600 kA cell design

M. Dupuis, Jonquière ; V. Bojareivs, Greenwich

In 2000, the author Mr Dupuis already presented the retrofit of a 300 kA into a 350 kA cell design, and then into a new 400 kA cell thermo-electric design [1] by extending the length of the potshell. Then in 2003, by further extending the length, and this time by also slightly increasing the potshell width, he presented a new 500 kA cell thermo-electric design [2]. Later in 2005, still extending the length of the 500 kA cell potshell, he presented a new 740 kA cell thermo-electric design, and claimed that there is no foreseeable limit to a cell size as far as the thermo-electric cell heat balance aspect of the cell design is concerned [3].

Finally in 2005/06, Mr Dupuis and Mr Bojareivs presented the MHD and the potshell mechanical design of the 500 and 740 kA cells claiming that there seems to be no foreseeable design limit to the cell size as regards the MHD and potshell mechanical aspects [4-6]. The recent increase in cell amperage in newly constructed smelters and prototypes, for example in China [7-9], confirms of this point of view.

In the meantime, over the last ten years, cell design has continued to evolve, especially as regards the cell lining design, so much so that a cell lining seen as best world practice ten years ago now appears old-fashioned, if not obsolete. This evolution clearly warrants a second retrofit study in order to incorporate the new best practice design ideas: using new or improved modelling tools, the aim is to boost the 500 kA cell design into a 600 kA cell design, while still keeping the same potshell and busbar.

Review of the 500 kA cell busbar designs: In diverse publications, the authors have presented three different busbar designs for the 500 kA cell. The first one is a 'classical' asymmetric busbar (Fig. 1) that auto-compensates for the return line [10]. The second one is a symmetric busbar (Fig. 2) with an external compensation busbar inspired by Pechiney 1987 patent [6, 11]. The third one is also a symmetric busbar (Fig. 3), but it uses a different configuration for the compensation busbar [6].

All three busbar designs have been re-analysed using an upgraded version of MHD-Valdis, the stability analysis code. This upgraded version takes into account the presence of the open bath channels, and is hence better at predicting the shape of the bath-metal interface [12]. There is little change in the calculated vertical component of the magnetic fields (B_z) and in the stability prediction as compared to previously presented results. But the predicted bath-metal interface deformation is now significantly different.

New anode stub hole TEM model and anode design: The new anode stub hole thermo-electro-mechanical (TEM) model presented in [13] has been used to calculate what would be the anode voltage drop of a 1.95 m long by 0.665 m wide anode. This anode has 4 stubs of 175 mm diameter and incorporates a new type of stub hole design. There are 48 such anodes in the 500 kA cell design. In Fig. 4, the 1/16 TEM anode stub hole model predicts a voltage drop of 214 mV from the bottom of the anode carbon block to the top of the stub. The obtained average contact resistance is then fed to the standard, half anode thermo-electric (TE) model, which in turn predicts 265 mV for the total anode voltage drop from the clamp connection to the bottom of the anode carbon block (Fig. 5).

New cathode collector bar slot TEM model and cathode design: The new cathode collector bar slot TEM model presented in [14] has been used to calculate what would be the cathode voltage drop of a 4.17 m long by 0.665 m wide and 0.58 m high fully graphitized cathode block. That cathode block has two collector bar slots and uses 220 mm high by 140 mm wide collector bars

each containing a big copper insert [15]. There are 24 such cathode blocks in the 500 kA cell design. The TEM model predicts that the cathode voltage drop will only be 87 mV, as can be seen in Fig. 6.

The resulting average contact resistances are then fed into the standard cathode side slice TE model of the same electrical design. Of course such a different design requires some adjustment of the thermal lining in order to prevent the top edge of the block becoming too cold and hence being covered by ledge way past the anode shadow. The cathode side slice TE model is the perfect tool to work on those adjustments.

Another change has been made to the cathode lining design to accommodate a still longer anode: the 100+ mm thick silicon carbide sidewall was replaced by a now standard 70 mm thick silicon carbide sidewall. As we can see from the calculated isotherms in Fig. 7, the model predicts a ledge profile that is quite acceptable at a typical cell superheat.

Full cell quarter model including the liquid zone: At this stage of a retrofit study, it would be common practice to develop a full cell slice model (see for example Fig. 2 of [3]). In the current study, that step was bypassed in order to develop directly a full cell quarter model including the liquid zone (see model mesh in Fig. 8). This model allows us to predict the ledge profile all around the perimeter of the cell, but letting the model converge to predict the ledge profile requires a lot of CPU time. In the current study, we used the quarter cell model including liquid zone to compute what the current density would be in the metal pad if we used big copper inserts in the collector bars, assuming the initial ledge profile (see Fig. 9). With these copper inserts, there is practically no horizontal current in the metal pad, even in this fairly wide cathode design.

Calculation of the retrofitted cell amperage using Dyna/Marc: There are many ways to carry out a retrofit study. In [1-3], each incremental step was an operable design at the quoted amperage. This is the standard way to work when using Dyna/Marc 'What if' panel as each solution is by definition in perfect thermal balance.

In the current study, the procedure is different: TEM models were used so as to reduce the anode and cathode electrical resistance, but without considering how this affects the cell thermal balance. Then the half anode and cathode side slice TE models were used to assess that thermal impact and to calculate what would be the total cell heat loss at a typical cell superheat. So at this stage of the study, a 1.95 m long anode is expected to operate at an average of 265 mV of voltage drop at 500 kA and the total anode panel should lose 420 kW according to the half anode TE model.

According to the cathode side slice TE model, the cathode is expected to operate with a 87 mV of voltage drop and to lose 665 kW if operated at 500 kA and 7°C of superheat. Yet, no calculations were done up to now to predict the internal heat of the cell, so as to verify whether the cell can really be in perfect thermal balance under these conditions (500 kA and 7°C of superheat, with a typical 4 cm of anode to cathode distance (ACD) per example, which was considered the best practice value ten years ago). In fact, even without making any calculations, it should be obvious to any experienced cell designer that this will not be the case!

Since that time, slotted anodes have become common, and these have allowed cells to operate at 3.5 cm ACD, as calculated by the same voltage break down equations [16]. So, not only have the anode and cathode electrical resistances decreased with the retrofitted cell design, but the bath electrical resistance is now significantly lower as well. Furthermore, by reducing the thickness of the silicon carbide sidewalls to 70 mm, we have made room to accommodate 2.0 m long anodes while still maintaining a comfortable 280 mm wide anode to sidewall distance (ASD).

The task at this stage is to enter all that information into Dyna/Marc and to ask: at what amperage does that cell design need to operate in order to be in perfect thermal balance at a typical cell superheat? As can be seen in Fig. 10, the Dyna/Marc answer to that question is 600 kA.

Verification of the thermal balance at 600 kA using the ANSYS® based TE models: Dyna/Marc is the perfect tool to get a quick answer to difficult questions like the one asked above; but this answer cannot be accepted as final. It is safe standard practice to double check this Dyna/Marc prediction using the more accurate ANSYS® finite element based TE models. The model can be either a full cell slice model or, as in this current study, can combine models of separate half anode and cathode side slice.

The half anode model predicts that 48 2.0 m long anodes in a cell operated at 600 kA will have an average anode drop of 318 mV, and they will dissipate 449 kW with a 10 cm thick cover. The cathode side slice model predicts that if operated at 600 kA and 7°C of superheat, then the cathode drop would be 104 mV and the cathode would dissipate 676 kW, while maintaining a comfortable ledge profile.

Since the internal heat at 600 kA, (which corresponds to an anodic current density of 0.94 A/cm² and 3.5 cm ACD), according to Dyna/Marc will be 1,140 kW, the cell should be in perfect thermal balance quite close to those assumed operating conditions. Note that Dyna/Marc also predicts 96.4% current efficiency (CE) and 4.29 V, which corresponds to a energy consumption of 13.3 kWh/kg Al.

Verification of the the MHD stability at 600 kA using MHD-Valdis: The final verification to make is that the cell will still be stable when operated at 600 kA without any modification of the busbar. The answer may depend on the type of busbar design selected for the base case 500 kA cell technology. An asymmetric busbar designed to auto-compensate a 500 kA return line will not be able to perfectly compensate a 600 kA return line, and that will for sure reduce the cell stability.

Yet a very good busbar design is able to accommodate a lot of amperage creep, as we learned from the evolution of the AP30 cell technology over the last 20 years. The busbar was initially designed to operate at 280 kA, and yet that same busbar now supports cell operation at 360-380 kA, still without major impact on the cell stability. Clearly there is some built-in robustness in a good busbar design!

Nevertheless, a busbar design incorporating independent compensation busbars is more flexible as it allows separately adjustment of the current running in the compensation loop(s). Suitable adjustments can perfectly compensate for increased return line current. Fig. 11 shows results for the third busbar design, this time with a cell operating at 600 kA instead of 500 kA . This demonstrates that, despite the amperage increase the B_z is still more or less the same once the amperages in the compensation loops are adequately readjusted.

Note that the ACD has not been readjusted between the 500 kA and the 600 kA runs of the MHD cell stability analysis. This is because we assume that it is the use of slotted anodes that leads to a smaller calculated ACD and so changes the internal heat generation. The physical ACD that matters in terms of cell stability we assume remains the same in the 500 kA cell design (using the old conventional unslotted anodes) as in the 600 kA cell design (using slotted anodes).

Conclusions

This demonstration study shows how to retrofit a ten years old 'past prime if not obsolete' 500 kA cell technology to make it an up-to-date 'innovative' 600 kA cell technology. It highlights the huge potential capacity creep that is present in even fairly recent cell designs. A more concrete example is the recently published results of the DX cell technology, which now operates at 370 kA, while designed only a few years ago to operate at 340 kA [17, 18].

The authors also hope that this demonstration study will highlight the value of using mature state-of-the-art mathematical models to carry out such studies. Those exact same models, used by the majority of the groups actively developing high amperage cell technology today, are available to the whole aluminium industry through GeniSim Inc.

References

- [1] M. Dupuis, Thermo-Electric Design of a 400 kA Cell using Mathematical Models: A Tutorial, *Light Metals*, TMS, (2000), 297-302.
- [2] M. Dupuis, Thermo-Electric Design of a 500 kA Cell, *ALUMINIUM* 79(7/8) (2003), 629-631.
- [3] M. Dupuis, Thermo-Electric Design of a 740 kA Cell, Is There a Size Limit, *ALUMINIUM* 81(4) (2005), 324-327.
- [4] M. Dupuis and D. Richard, Study of the Thermally-Induced Shell Deformation of High Amperage Hall-Héroult Cells, *Proceedings of the 4th Conference on Light Metal*, COM, (2005), 35-47.
- [5] M. Dupuis, and V. Bojarevics, Comparing the MHD cell stability of an aluminium reduction cell at different metal pad height and ledge thickness, *COM*, (2006), 479-497.
- [6] M. Dupuis, V. Bojarevics and D. Richard, MHD and pot mechanical design of a 740 kA cell *Aluminium* 82, (2006) 5, 442-446.
- [7] Qi, X. et al., Successful commercial operation of NEUI400 potline, *Light Metals*, TMS, (2010), 359-363.
- [8] D. Lv et al., New progress on application of NEUI400 aluminium reduction cell technology, *Light Metals*, TMS, (2011), to be published.
- [9] D. Lv et al., Development of NEUI500 high energy efficiency aluminium reduction cell technology, *Light Metals*, TMS, (2011), to be published.
- [10] M. Dupuis and V. Bojarevics, Weakly Coupled Thermo-Electric and MHD Mathematical Models of an Aluminium Electrolysis Cell, *Light Metals*, TMS, (2005), 449-454.
- [11] J. Chaffy, B. Langon and M. Leroy, Device for Connection Between Very High Intensity Electrolysis Cells for the Production of Aluminium Comprising a Supply Circuit and an Independent Circuit for Correcting the Magnetic Field, US patent no 4,713,161, (1987).
- [12] V. Bojarevics and K. Pericleous, Solution for the metal-bath interface in aluminium electrolysis cells, *Light Metals*, TMS, (2009), 569-594.
- [13] M. Dupuis, Development and application of an ANSYS based thermo-electro-mechanical anode stub hole design tool, *Light Metals*, TMS, (2010), 433-438.
- [14] M. Dupuis, Development and application of an ANSYS based thermo-electro-mechanical collector bar slot design tool, *Light Metals*, TMS, (2011), to be published.
- [15] G. E. Homley, and D. P. Ziegler Cathode collector bar, US patent no 6,231,745, (2001).
- [16] M. Dupuis and H. Côté, *Dyna/Marc 1.9 User's guide*, (2006).

[17] A. Kalban, et al., 2008: A milestone in the development of the DX technology, Light Metals, TMS, (2009), 359-363.

[18] A. Zarouni et al., DX pot technology powers green field expansion, Light Metals, TMS, (2010), 339-348.

Authors

Dr. Marc Dupuis is a consultant specialised in the applications of mathematical modelling for the aluminium industry since 1994, the year when he founded his own consulting company GeniSim Inc (www.genisim.com). Before that, he graduated with a Ph.D. in chemical engineering from Laval University in Quebec City in 1984, and then worked ten years as a research engineer for Alcan International. His main research interests are the development of mathematical models of the Hall-Héroult cell dealing with the thermo-electric, thermo-mechanic, electro-magnetic and hydrodynamic aspects of the problem. He was also involved in the design of experimental high amperage cells and the retrofit of many existing cell technologies.

Dr. Valdis Bojarevics is reader in magnetohydrodynamics at the University of Greenwich (UK). He specialises in the numerical modelling of various electrometallurgical applications involving complex interactions of the fluid flow, thermal and electrical fields, melting front and free surface dynamics; he has been involved in numerous industrial consulting projects.

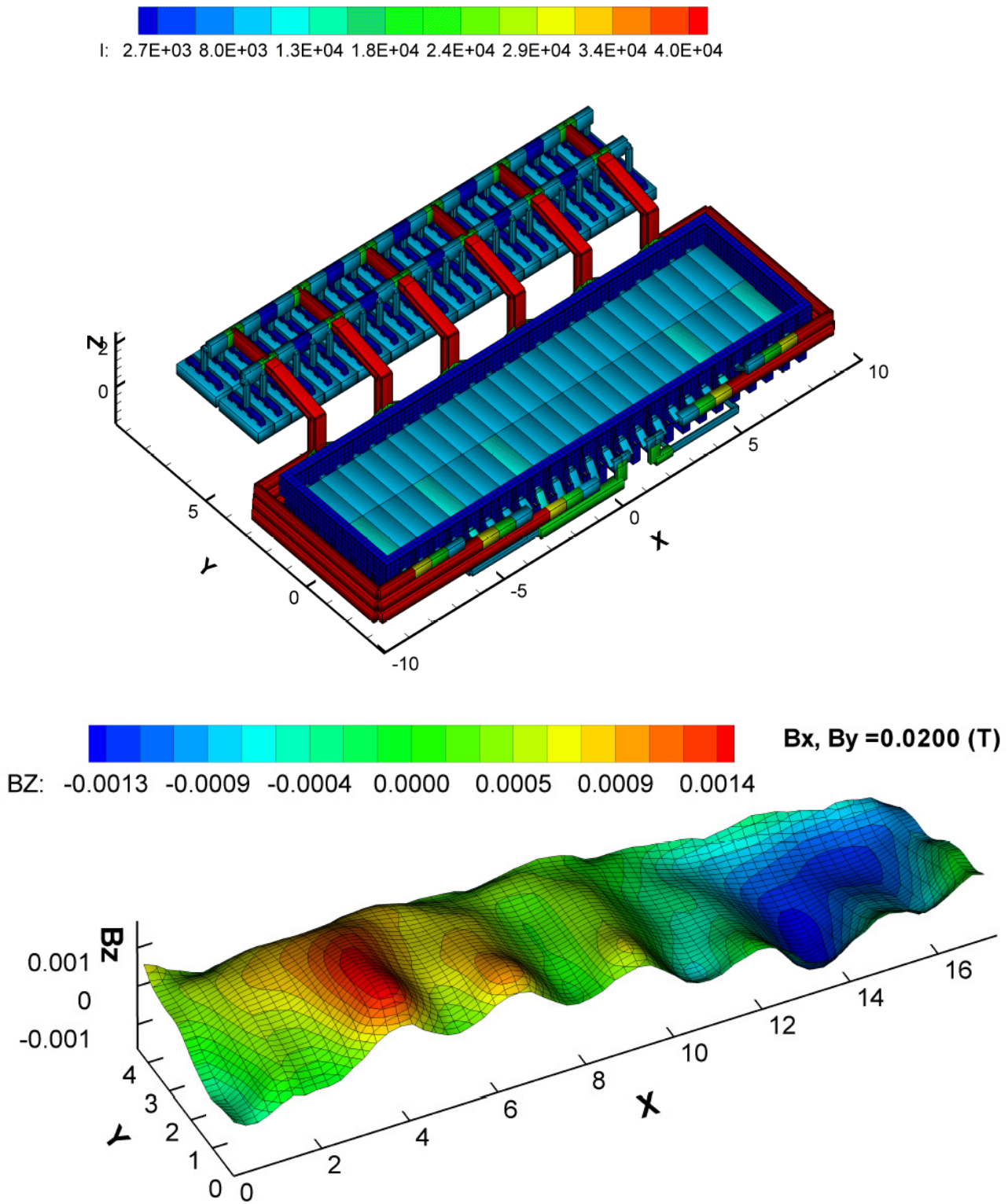


Figure 1: MHD-Valdis results for the asymmetric busbar design of the 500 kA cell

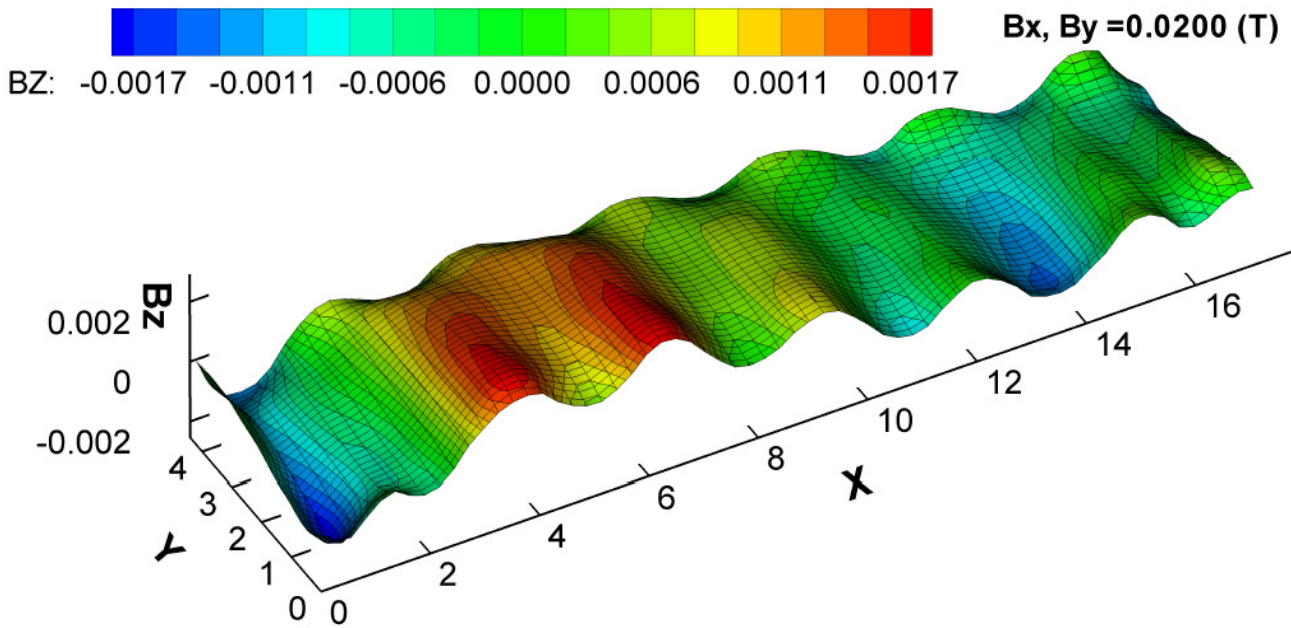
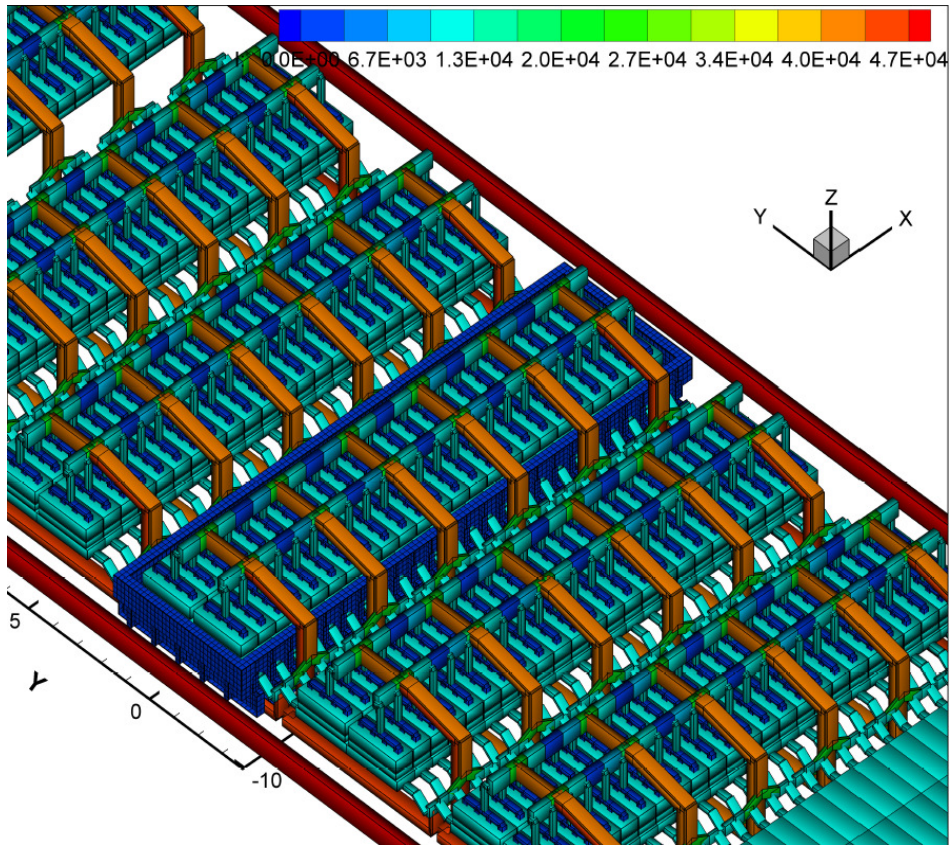


Figure 2: MHD-Valdis results for the Pechiney 1987 inspired busbar design of the 500 kA cell

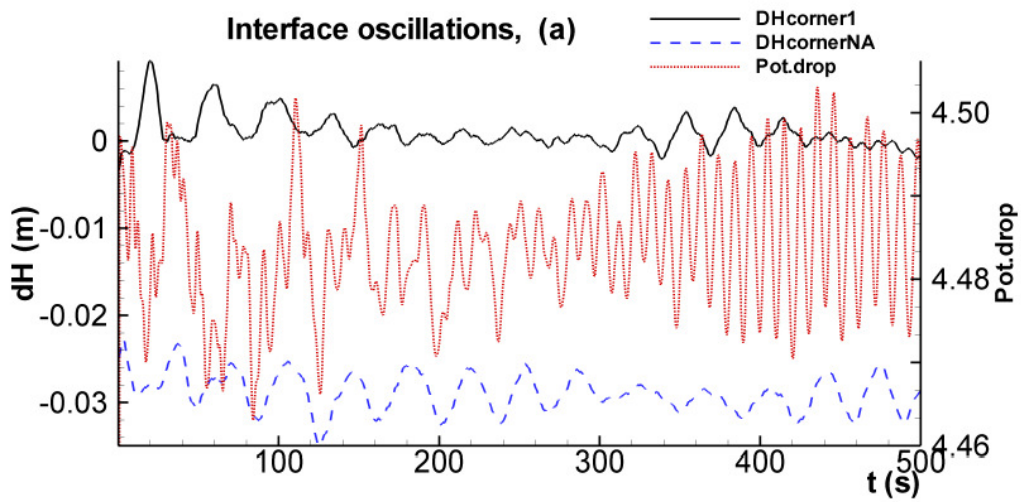
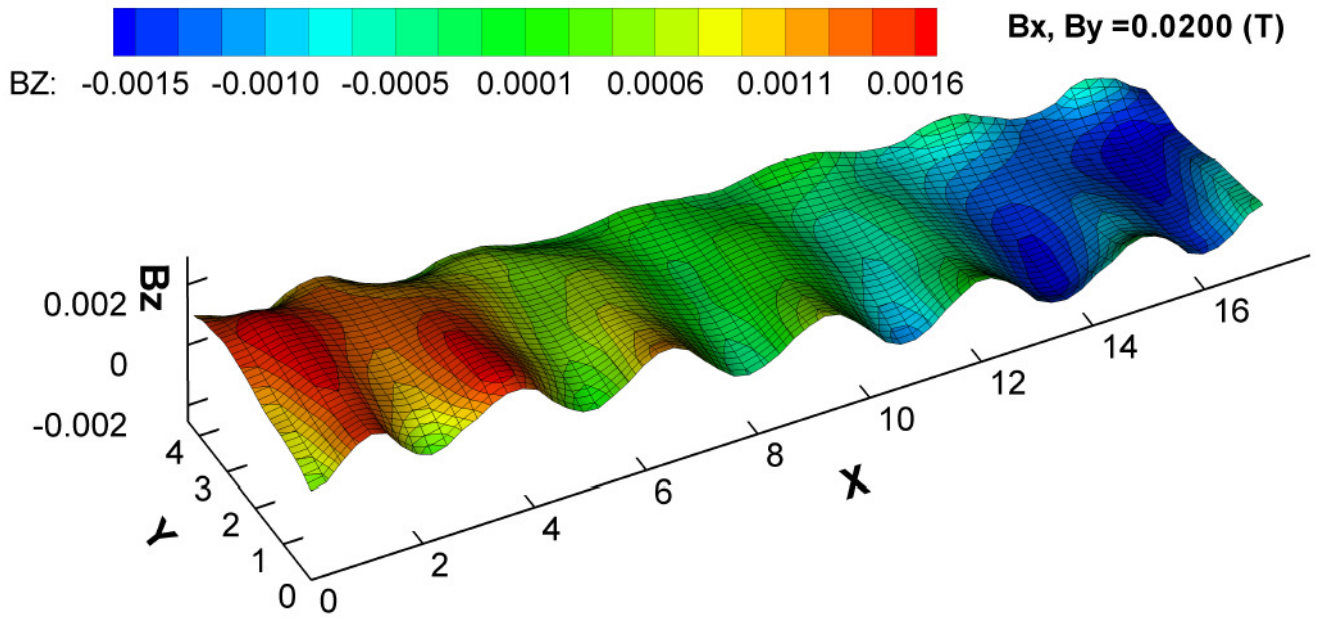


Figure 3: MHD-Valdis results for the alternative compensation busbar design of the 500 kA cell

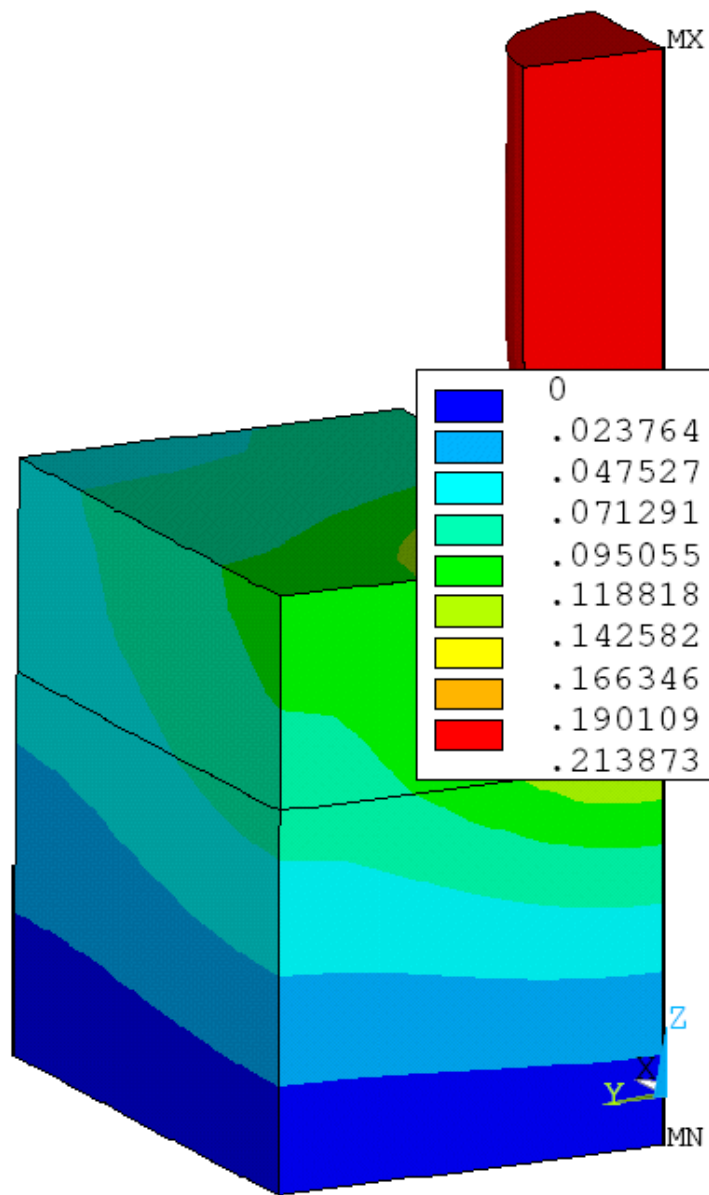


Figure 4: Predicted anode voltage drop from the anode stub hole TEM model at 500 kA

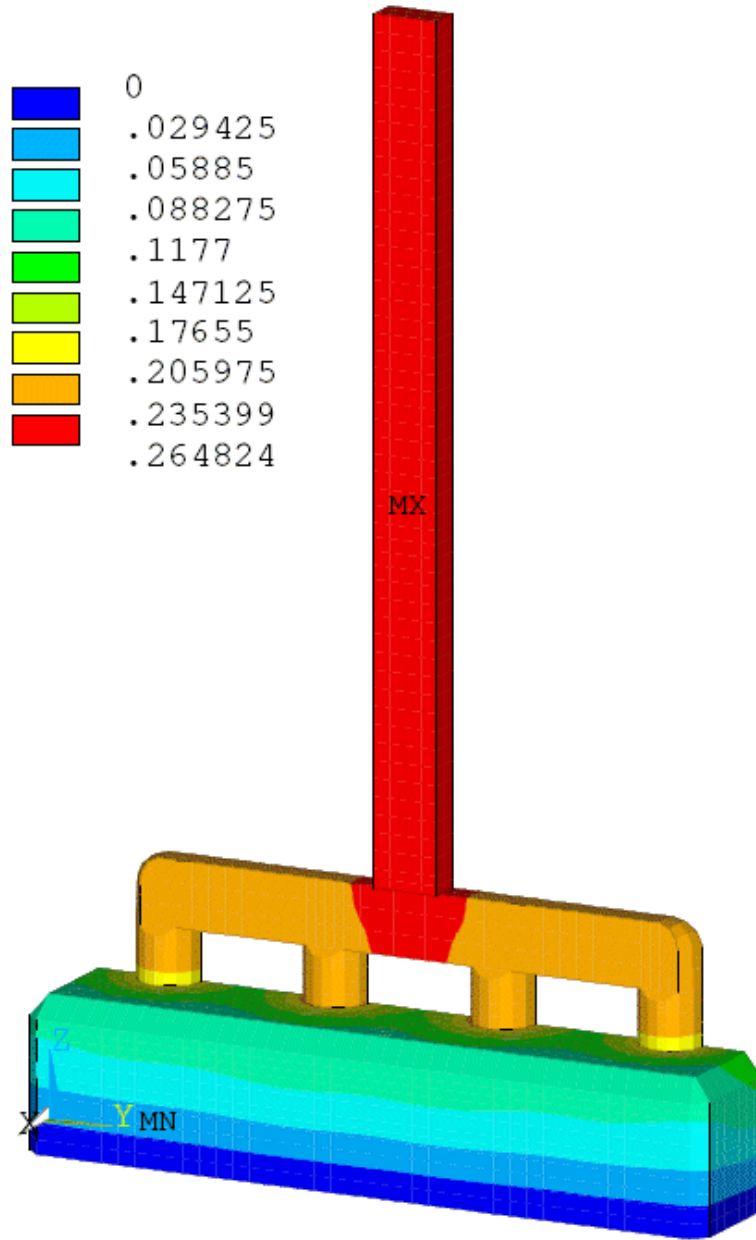


Figure 5: Predicted anode voltage drop from the half anode TE model at 500 kA

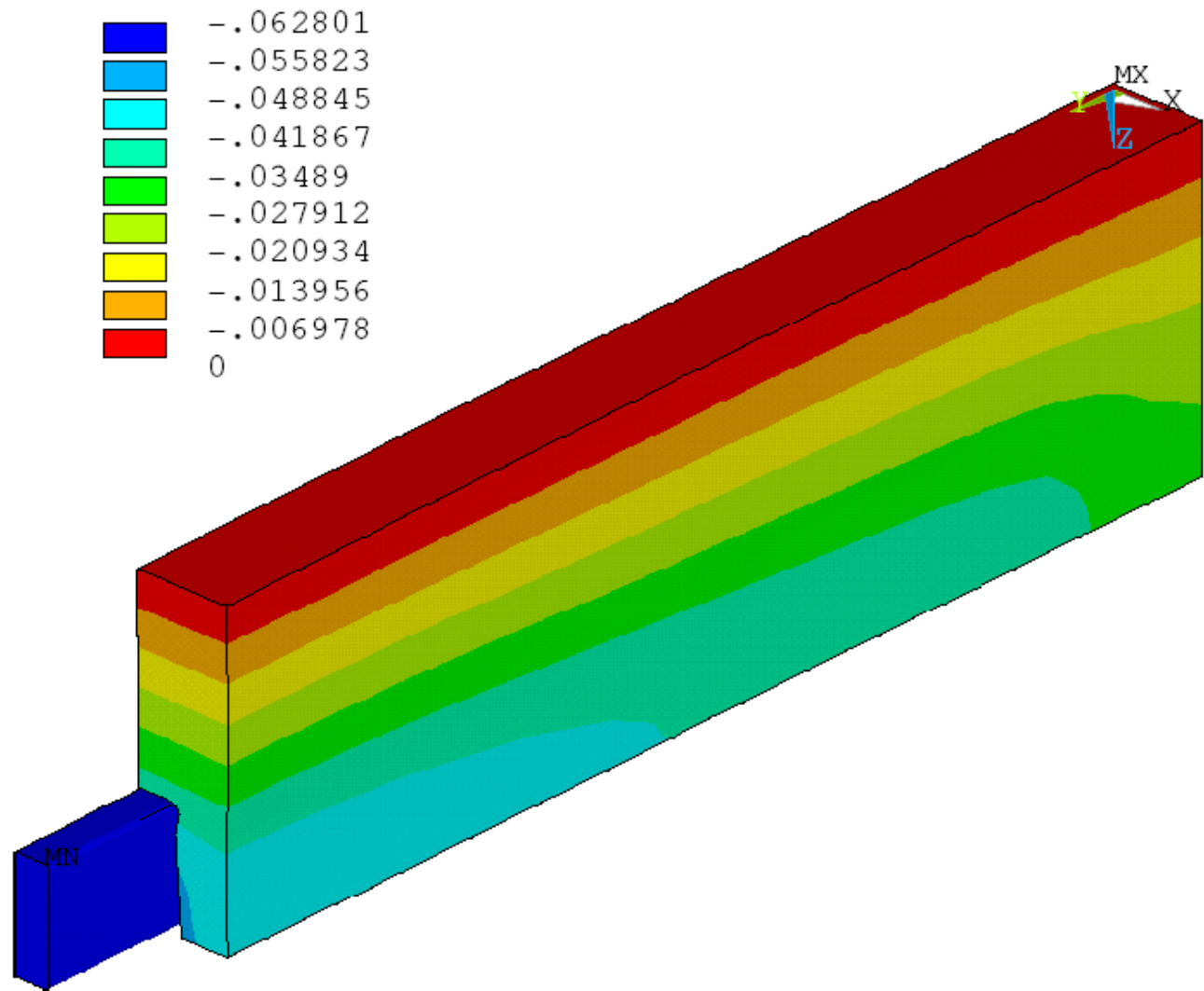


Figure 6: Predicted cathode voltage drop from the cathode collector bar slot TEM model at 500 kA

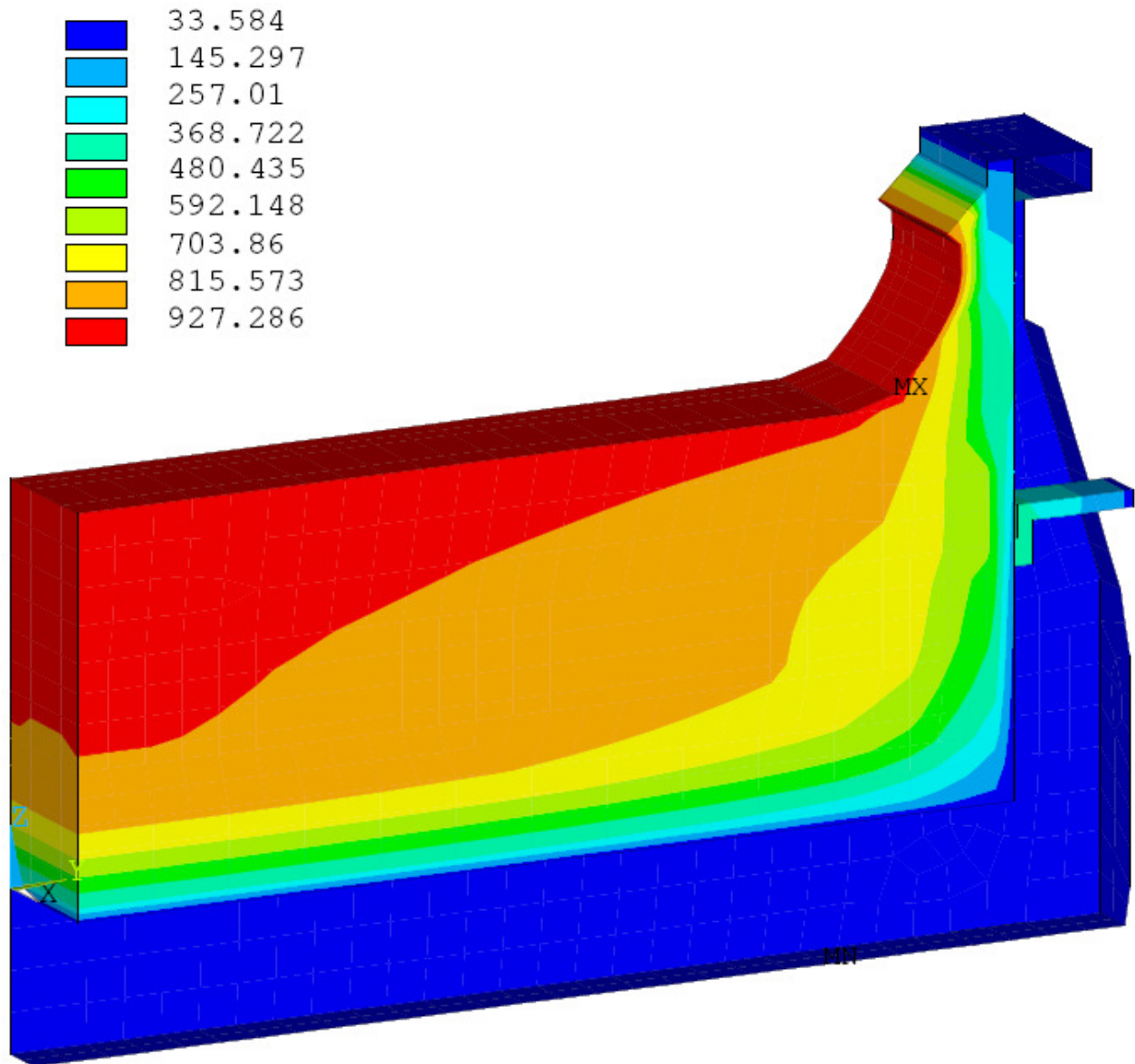


Figure 7: Predicted isotherms from the cathode side slice TE model at 500 kA

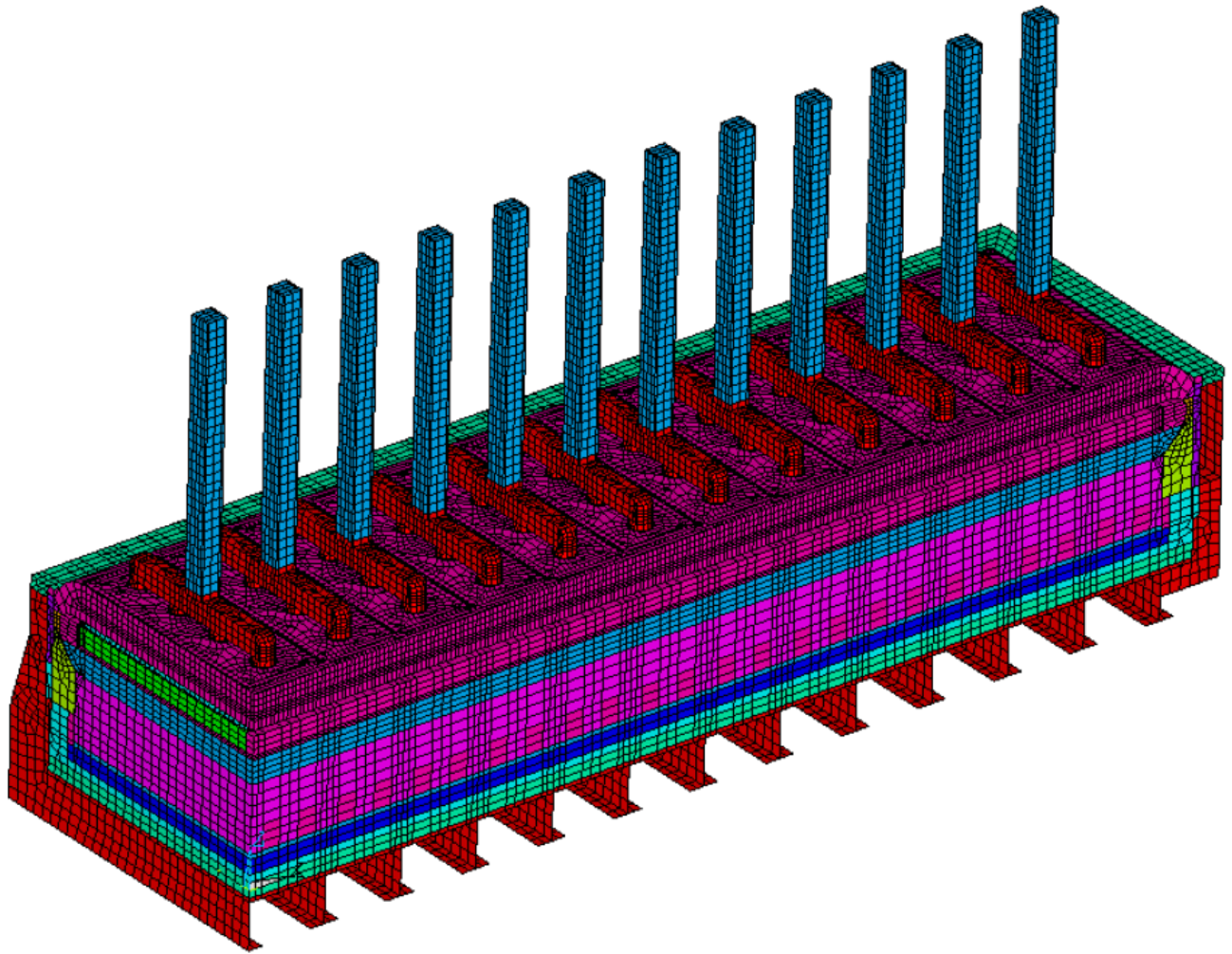
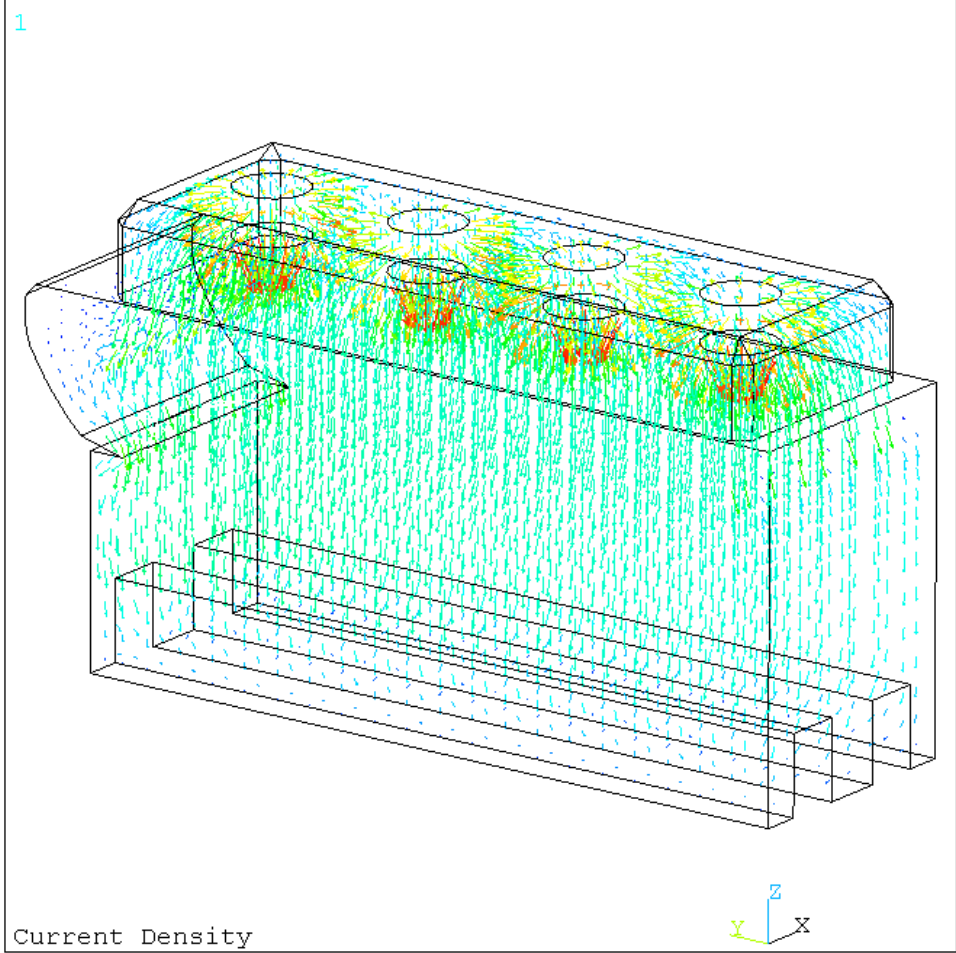


Figure 8: Mesh of the full quarter cell TE model including the liquid zone

1



ANSYS 12.0.1
OCT 21 2010
10:22:54
VECTOR
STEP=2
SUB =1
TIME=2
CD
ELEM=6900
MIN=311.758
MAX=19663

| | |
|---|---------|
| ■ | 311.758 |
| ■ | 1370 |
| ■ | 2428 |
| ■ | 3487 |
| ■ | 4394 |
| ■ | 5452 |
| ■ | 6510 |
| ■ | 7417 |
| ■ | 8476 |
| ■ | 9534 |
| ■ | 10441 |
| ■ | 11499 |
| ■ | 12558 |
| ■ | 13465 |
| ■ | 14523 |
| ■ | 15581 |
| ■ | 16488 |
| ■ | 17547 |
| ■ | 18605 |
| ■ | 19663 |

Figure 9: Current density close to the centerline predicted by the full cell quarter model at 500 kA

DYNA/MARC 1.95 - [VAWm19]

File Process Controller Operator Run List Windows Language Help

DYNA/MARC 1.95 - [VAWm19]

Demo example of a prebaked PBF cell inspired from VAW's JOM paper
 liquidus superheat, 3.5 cm ACD, 2 m anode length, 12.0% AlF₃, 600 kA
 HC10 4.17m cathode block, top 7 cm bottom 7 cm SiC side block
 10 cm cover over anodes, 17.5 cm stud diameter, 4 studs per anode
 48 anodes, 24 cathode blocks, 17.8 m X 4.85 m inside potshell size

Date Created : 8/2/99 Last Modified : 10/12/10

Steady State Solution

| Variable | Value | Units |
|-------------------------------------|----------|-------------|
| Cell amperage | 600.0 | [kA] |
| Anode to cathode distance | 3.50000 | [cm] |
| Operating temperature | 963.899 | [C] |
| Ledge thickness, bath level | 5.37447 | [cm] |
| Ledge thickness, metal level | 1.68353 | [cm] |
| Anode beam position | 0.0000 | [cm] |
| Mass of metal | 33458.9 | [kg] |
| Mass of bath | 9739.88 | [kg] |
| Mass of dissolved alumina | 243.497 | [kg] |
| Mass of dispersed alumina | 110.829 | [kg] |
| Mass of alumina sludge | 4.1933 | [kg] |
| Mass of dissolved aluminum fluoride | 1168.785 | [kg] |
| Mass of dispersed aluminum fluoride | 1.081 | [kg] |
| Mass of aluminum fluoride sludge | 0.0003 | [kg] |
| Mass of calcium fluoride | 584.393 | [kg] |
| Mass of lithium fluoride | 0.000 | [kg] |
| Mass of magnesium fluoride | 0.000 | [kg] |
| Alumina feeding rate | 374.187 | [kg/hr] |
| Aluminum fluoride feeding rate | 2.46778 | [kg/hr] |
| Target cell resistance | 4.40157 | [micro-ohm] |

Steady State derived Variables

| Variable | Value | Units |
|--|----------|---------|
| Rate of change of: | | |
| ACD | -0.02987 | [cm/hr] |
| Operating temperature | 0.0000 | [C/hr] |
| Ledge thickness, bath level | 0.000 | [cm/hr] |
| Ledge thickness, metal level | 0.000 | [cm/hr] |
| Mass of dispersed Al ₂ O ₃ | 0.000 | [kg/hr] |
| Mass of Al ₂ O ₃ sludge | 0.00000 | [kg/hr] |
| Mass of dissolved Al ₂ O ₃ | 0.0000 | [kg/hr] |

DYNA/MARC: What If

List of Design Variables

| Variable | Design Value | Units | Set as Target |
|------------------------------------|--------------|---------------------|----------------------------------|
| Anode to Cathode Distance | 3.5 | cm | <input type="radio"/> |
| Cell Amperage | 600 | kA | <input type="radio"/> |
| Conc. of Excess Aluminum Fluoride | 12 | % | <input type="radio"/> |
| Concentration of Dissolved Alumina | 2.5 | % | <input type="radio"/> |
| Concentration of Calcium Fluoride | 6 | % | <input type="radio"/> |
| Concentration of Lithium Fluoride | 0 | % | <input type="radio"/> |
| Conc. of Magnesium Fluoride | 0 | % | <input type="radio"/> |
| Bath Level | 20 | cm | <input type="radio"/> |
| Bath Ledge Heat Transfer Coef. | 1425 | W/m ² °C | <input type="radio"/> |
| Metal Ledge Heat Transfer Coef. | 2052 | W/m ² °C | <input type="radio"/> |
| Metal Level | 20 | cm | <input type="radio"/> |
| Anode Length | 2 | m | <input type="radio"/> |
| Cavity Length | 17.48 | m | <input type="radio"/> |
| Anode Panel Heat Loss | 423 | kW | <input type="radio"/> |
| Cathode Bottom Heat Loss | 240 | kW | <input type="radio"/> |
| Cell Operating Temperature | 963 | °C | <input checked="" type="radio"/> |
| Anode Voltage Drop | 318 | mV | <input type="radio"/> |
| Cathode Voltage Drop | 104.4 | mV | <input type="radio"/> |
| Anode Width | 0.665 | m | <input type="radio"/> |
| Cavity Width | 4.55 | m | <input type="radio"/> |

Run Exit

Press F1 for Help Demo example of a prebaked PBF cell inspired from VAW's JOM paper 10/21/10 12:10 PM CAPS NUM INSERT

Figure 10: Dyna/Marc steady-state solution as calculated using the “What if” panel

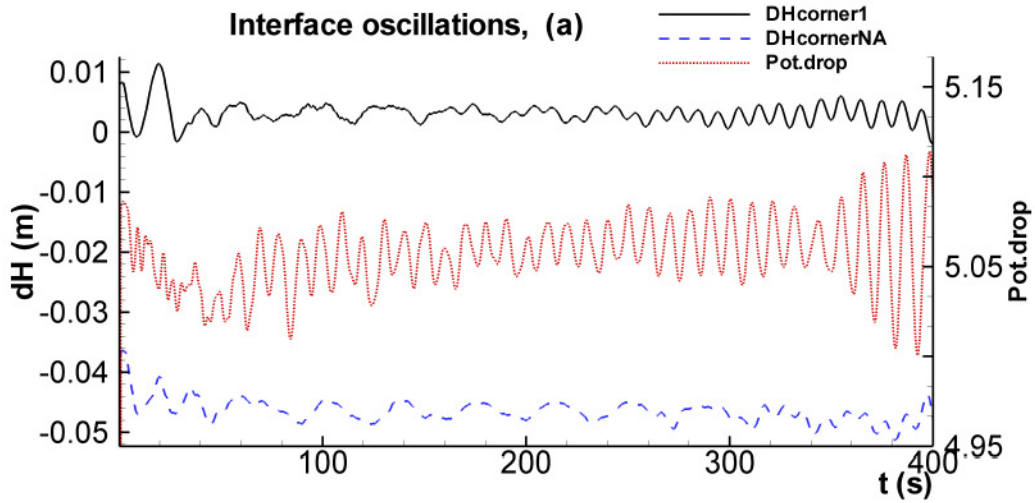
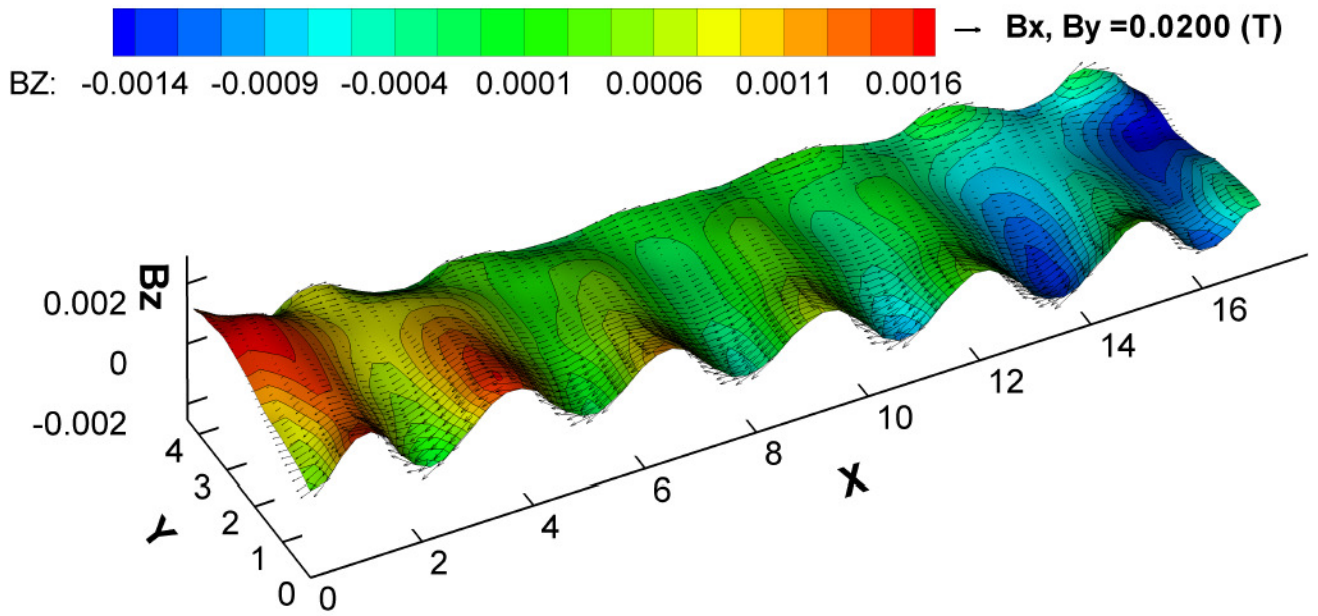


Figure 11: MHD-Valdis results for the alternative compensation busbar design of the 600 kA cell